1   The role of chemical design on the performance of organic semiconductors Hugo Bronstein[1],
2   Christian B. Nielsen[2], Bob C. Schroeder[3], Iain McCulloch[4,5]

3   1. University of Cambridge, UK
4   2. Queen Mary University of London, UK
5   3. University College London, UK
6   4. Imperial College London, UK
7   5. King Abdullah University of Science and Technology, Kingdom of Saudi Arabia
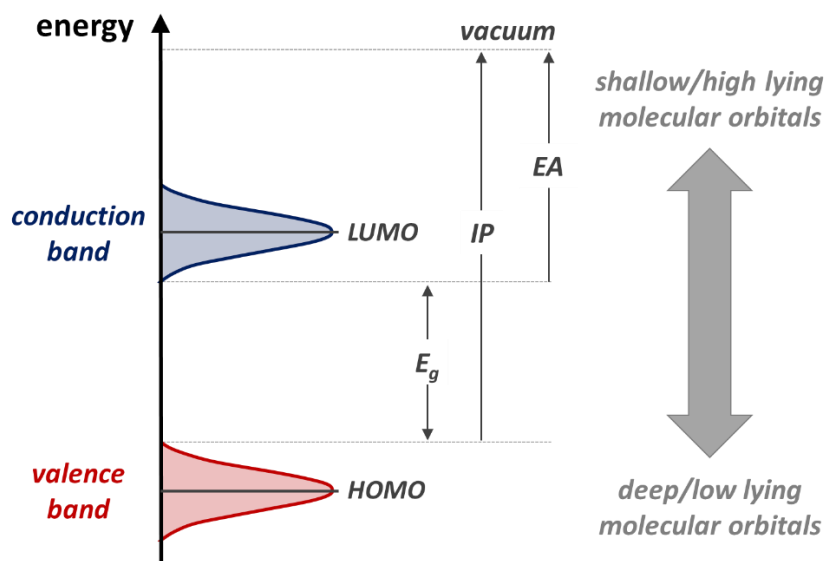
8

Introduction

10   Organic semiconductors are increasingly utilised as the active layer in a wide range of new
11   technologies, arising from their solution processability, light-weight and flexibility. The versatility of
12   synthetic organic chemistry drives the development of applications benefiting from such properties,
13   including biological sensing, wearable electronics, semi-transparent photovoltaics and flexible
14   displays. Advances in these applications are underpinned not only by developments in chemistry but
15   also by a deeper understanding of the factors that govern the properties of the material through the
16   continuous improvement of analytical and computational techniques. Judicious molecular design
17   provides control of the semiconductor frontier molecular orbital energy distribution and guides the
18   hierarchical assembly of organic semiconductors into functional films where we can control the
19   properties and motion of charges and excited states. This review aims to illustrate how chemistry and
20   molecular design play integral roles in advancing electronic device properties in the main and
21   emerging applications of organic semiconductors.

22

Molecular Orbital Design Considerations

24   The frontier molecular orbital energy levels and their distribution along the conjugated pi electron
25   skeleton of the molecule (both small molecule and polymer) play a critical role in intra and
26   intermolecular charge transport, light absorption, light emission, charge injection/extraction, charge
27   trapping, and ambient electrochemistry. The highest occupied molecular orbital (HOMO) energy level
28   is largely dependent on the electron density and delocalisation of the conjugated π-electron system.
29   Functional groups which can directly donate electron density either mesomerically (i.e. lone pair
30   donation from nitrogen, oxygen, sulfur) or inductively (i.e. alkyl chains) can contribute to raising the
31   HOMO energy level, i.e. decreasing the solid-state ionisation potential. Conversely electron
32   withdrawing groups, such as fluorine, carbonyl groups or cyano groups, can act to both lower the
33   HOMO energy level, whilst also stabilising the lowest unoccupied molecular orbital (LUMO) energy
34   level, corresponding to an increase in the solid-state electron affinity. When considering
35   intermolecular electronic coupling, the spatial distribution of the molecular orbital density is essential,
36   in order to maximise π-orbital overlap along the conjugated system. A practical illustration of the
37   manipulation of molecular orbital energy levels is shown in the Tutorial Box, with the example of the
38   systematic functionalisation of a fluorene benzothiadiazole rhodanine conjugated molecule.
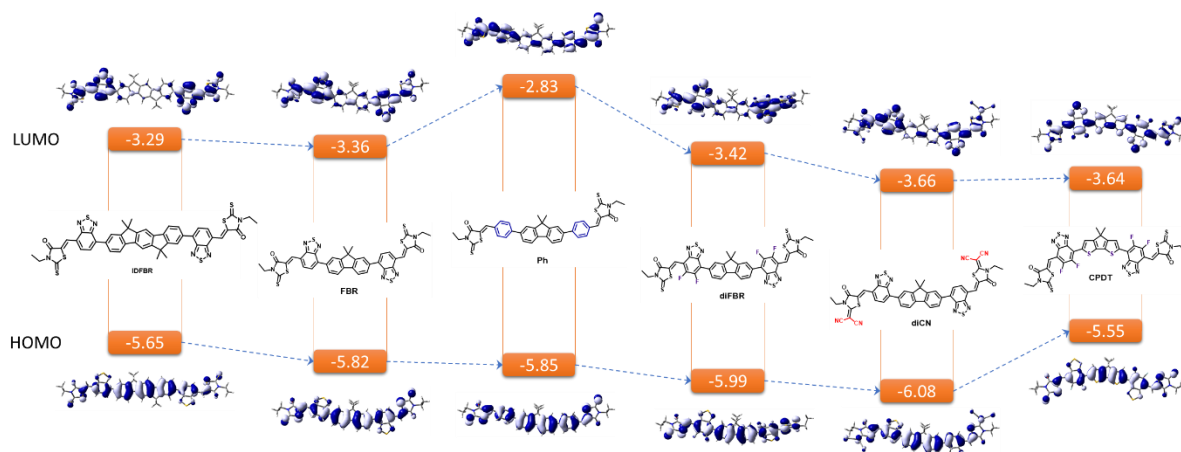
39

40

TUTORIAL BOX 1. Definition of terminology used to describe molecular orbital energy levels.

42

The figure of Tutorial Box 1. Illustrates the energies relevant to the molecular orbital design of organic semiconductors. The discrete HOMO and LUMO molecular energy levels observed in isolated organic semiconductor molecules, are broadened into electronic bands, the valence and conduction band. The optical band gap (E_g) is defined as the energy gap between the highest energy of the valence band and the lowest energy of the conduction band. The ionisation potential (IP) is the energy needed to remove one electron from the top of the valence band, whereas the electron affinity (EA) is defined as the energy from the bottom of the conduction band to the vacuum level.

50

TUTORIAL BOX 2. Case study in frontier energy level manipulation through molecular design.

[FOOTNOTE: Frontier energy levels (all in eV) and molecular orbital distributions have been estimated using density functional theory. The ground state geometries were obtained by B3LYP density functional method with basis set def2-SVP. The dispersion correction was conducted by Grimme's D3 version with the BJ damping function. The excited states of target molecules on ground state structures were calculated by TD-DFT with the same level. The systematic name of FBR is 5,5'-(((9,9-

58 dimethyl-9*H*-fluorene-2,7-diyl)bis(benzo[*c*][1,2,5]thiadiazole-7,4-diyl))bis(methanylylidene))bis(3-
59 ethyl-2-thioxothiazolidin-4-one)]

60 TEXT FOR TUTORIAL BOX: As illustrated on the left of tutorial box 2, the HOMO energy level of the
61 non-fullerene acceptor IDFBR ((5*Z*,5'*Z*)-5,5'-(((6,6,12,12-tetramethyl-6,12-dihydroindeno[1,2-
62 *b*]fluorene-2,8-diyl)bis(benzo[*c*][1,2,5]thiadiazole-7,4-diyl))bis(methaneylylidene))bis(3-ethyl-2-
63 thioxothiazolidin-4-one)) is delocalised along the entire π-conjugated backbone, whereas the LUMO
64 is predominantly localised on the electron-deficient 2,1,3-benzothiadiazole (BT) and rhodanine
65 moieties.[1] Consequently, chemical modifications to modify the LUMO of the molecule need to be on
66 the periphery, while the HOMO is potentially tuned with chemical modifications on any conjugated
67 part of the molecule. Reducing the conjugation length therefore of the central indenofluorene core
68 to a fluorene unit (FBR) predominantly raises the HOMO energy level (by almost 0.2 eV) while there is
69 little shallowing of the LUMO (less than 0.1 eV). Substituting the BT moieties on FBR with phenylenes
70 (Ph) raises the LUMO significantly (~0.5 eV) due to the less electron-deficient nature of the phenylene
71 groups. The HOMO, on the other hand, is only marginally affected. Difluorination of the BT units (diFBR)
72 lowers both the HOMO and LUMO by 0.1 – 0.2 eV compared with FBR due to the electron withdrawing
73 inductive effects from the electronegative fluorine atoms. Introduction of the much stronger electron-
74 withdrawing dicyanovinyl moiety than the thiocarbonyl on the rhodanine (diCN) has a stronger effect,
75 lowering both HOMO and LUMO by approximately 0.3 eV relative to FBR. As well as electron density
76 considerations, the delocalisation of the pi orbital skeleton plays a significant role in the orbital energy
77 levels. FBR has a non-coplanar backbone conformation due to repulsive torsional interactions
78 between neighbouring hydrogens on the BT and fluorene units; these steric effects can be alleviated
79 with the replacement of the fluorene core with cyclopentadithiophene (CPDT), allowing more orbital
80 overlap and thus further raising the HOMO (in addition to the effect of the electron rich thiophene
81 rings) as well as lowering the LUMO. Further planarising S-F through electrostatic interactions are
82 possible between the lone pairs of electrons on the fluorine atoms of the diFBT, and the
83 electropositive sulfur atoms on the peripheral thiophene rings of the CPDT unit, with a consequent
84 additional lowering of the LUMO. An additional consequence of pi orbital delocalisation, is that the
85 LUMO molecular orbital now is now distributed more over the core of the molecule, and hence any
86 functionalisation of the core will affect the LUMO as well as the HOMO energy level. Although not
87 illustrated in the tutorial box, heteroatom substitution of the carbon bridging atom of the fluorene
88 unit (with silicon or germanium) surprisingly did not appear to influence either of the frontier
89 molecular orbital energies. Typically, incorporation of bridging heteroatoms promotes an increase in
90 the respective bond lengths of the central ring to accommodate the larger atoms. The resultant larger
91 C-C bond length linking the two aromatic rings, reduces the antibonding interactions that arise from
92 the HOMO orbital node between the rings, thus deepening the HOMO energy level. Similarly, there
93 was also not a noticeable effect of chalcogen substitution of the sulphur atoms on the CPDT unit. In
94 general, increasing the chalcogen atom size reduces ring aromaticity, through decreasing participation
95 of the chalcogen lone pair in the ring, as the chalcogen – carbon bond length increases. This enhances
96 the diene character of the ring, reducing aromatic stabilisation and thus increasing the HOMO energy
97 level, and a reduced bandgap [2].

98 Charge transport is sensitive to traps within the bulk, [3] therefore p-type materials benefit from a small
99 ionisation potential, where filling of deep traps is thermodynamically unfavourable. Similarly, n-type
100 materials benefit from a large electron affinity, where again there are less accessible charge traps.
101 Injection of holes from an electrode into the HOMO of a semiconductor is more energetically facile
102 when the electrode work function is close to, or preferably larger than, the ionisation potential of the
103 semiconductor. This allows for ohmic contact, with low contact resistance at the electrode-
104 semiconductor interface. Correspondingly, for electron injection, the electron affinity should be as

105 large as possible. Achieving *in operando* stability of OS devices relies on the suppression of reactions
106 of both the neutral and charged semiconductor species.[4] In order to prevent the most
107 thermodynamically favourable reactions (involving a combination of oxygen and water), it has been
108 predicted that a neutral p-type semiconductor should have an ionisation potential of greater than 4.9
109 eV.[4] One such example of ambient electrochemistry is the reduction of oxygen in the presence of
110 water to form hydroxide anions from the transfer of electrons from shallow HOMO semiconductors.
111 However, in operation, i.e. the hole polaron formed from deep HOMO semiconductors has the
112 opposite trend in reactivity and can oxidise ambient water for example. The activation barriers of
113 these forward and reverse reactions fortunately lead to overpotentials which allow many organic
114 semiconductors to exhibit reasonable shelf and operational stabilities. Electron transport is
115 particularly affected by ambient reactions, and in the same way as p-type semiconductors, preventing
116 electrochemical oxidation reactions of excited electrons delocalized within the LUMO is essential. To
117 accomplish this, the LUMO energy level must be deep enough, i.e. the electron affinity must be large
118 enough, to prevent the formation of, for example, superoxide radical anion from reaction of excited
119 electrons with hydrated oxygen complexes [5] (one of the most favourable electrochemical reactions),
120 or the reduction of water. These unwanted electrochemical processes can reduce charge transport,
121 but moreover also lead to further irreversible chemical reactions within the semiconducting structure.
122 Defining a precise electron affinity value that needs to be exceeded to prevent these redox reactions
123 requires consideration of the electrochemical overpotential of the reaction, and is also influenced by
124 morphology. There is literature evidence however, to suggest that an electron affinity of greater than
125 4 eV will suffice to suppress oxidation. [6].

126

127 **Organic Field Effect Transistors**

128 Charge transport in organic semiconducting polymers relies on a combination of intrachain polaron
129 conjugation, facilitated by the polymer backbone π-electron delocalisation, and intermolecular charge
130 hopping between adjacent chains, facilitated by thin film microstructure. A close packed hierarchical
131 assembly of polymer backbones, promoted by intermolecular interactions, is often the dominant
132 factor in the optimisation of charge carrier mobility. Many design motifs have been proposed to
133 facilitate intermolecular contacts. An early example was the micron scale, three dimensional ordering
134 achieved in thin films of poly[2,5-bis(3-alkylthiophen-2-yl)thieno[3,2-*b*]thiophene] (pBTTT), illustrated
135 in Figure 1a [7]. This morphology was described as ordered lamellar sheets comprised of π-stacked
136 conjugated pBTTT backbones, with registration in the out of plane direction directed by the side chain
137 interdigitation of vertically adjacent polymer chains. Interdigitation was made possible by the
138 conformationally tolerant, regular spacing of the side chains along the backbone, with optimal special
139 separation to ensure an ordered and close packed side chain density on interdigitation. This approach
140 was also subsequently exploited in a series of isoindigo polymers [8], where the analogy with biological
141 interactions invoked the description "molecular docking" to describe the possible locking of alkyl
142 chains into sterically empty regions along the polymer chain. Indeed, the cumulative Van der Waals
143 interactions between "inert" aliphatic side chains are likely the dominant interaction that templates
144 morphology and short contacts. Even though the degree of interdigitation exhibited by pBTTT is
145 extremely unusual, a close packed and regular alkyl distribution between backbones can act to not
146 only create ordered morphology, but reduce the local free volume, where unwanted species such as
147 water can reside, leading to charge trapping and subsequently a suppression of carrier mobility.

148 More recently, it has been identified that efficient intramolecular charge transport can be optimally
149 facilitated when the polymer backbone exhibits as low intrinsic energetic disorder as possible, and is
150 resilient to torsional fluctuations between adjacent monomer units [9] [10]. This is typically achieved by
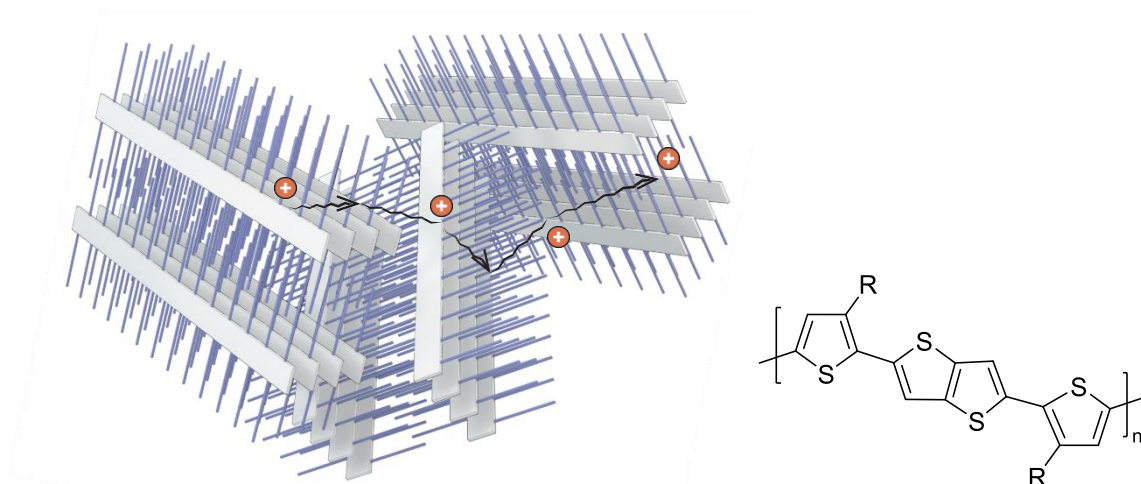
151   maximising the energetic barrier to rotation between aromatic repeat units along the backbone. There
152   are several molecular design strategies demonstrated to be successful in imparting co-planarity to a
153   conjugated backbone. The use of non-covalent through space interactions between adjacent ring
154   structures that can act as a barrier to rotation, thus promoting co-planarity. Common examples of this
155   approach include the electrostatic attractions between heteroatoms in close proximity to the linking
156   bond between aromatic units along the backbone. The sulphur atom on a linking thieno group, despite
157   the presence of two lone pairs of electrons, presents a partially positive charge due to the donation
158   of one lone pair to complete an aromatic ring. As a result, heteroatoms with available lone pairs of
159   electrons, such as oxygen and nitrogen can form strong attractive interactions with the sulphur, thus
160   rigidifying the linking bond. [11-13] This has specifically been exploited in the coupling of a thiophene ring
161   with a 3-alkoxythiothene unit. Bis-lactam based building blocks, like diketopyrrolopyrrole (DPP) and
162   isoindigo, on the other hand rely on more traditional hydrogen bonding-like interactions as evidenced
163   from their crystal structures.[14,15] The oxygen in the electron deficient lactam core and the hydrogen
164   atoms in close proximity to introduce conformational locks along the polymer backbone thereby
165   reducing rotational disorder and maximising orbital overlap. (Figure 2) Non-covalent stabilising
166   approaches were also exploited to design highly coplanar copolymers with low energetic disorder such
167   as the copolymer indacenodithiophene-co-benzothiadiazole (IDT-BT) [9], illustrated in Figure 1b. The
168   dominant planarising interaction in this case is a non-traditional hydrogen bond between the nitrogen
169   of the benzothiadiazole and the alpha hydrogen of the adjacent indacenodithiophene group. These
170   strong interactions overcome the repulsive steric exchange energies, giving rise to an extremely low
171   energetic disorder in this polymer. Despite a lack of long-range order, the assembly of side chains
172   promotes intermittent short contacts along the backbone. Transport is primarily one dimensional
173   along the backbone, with occasional hops between chains. As a result, these "short contact" polymers
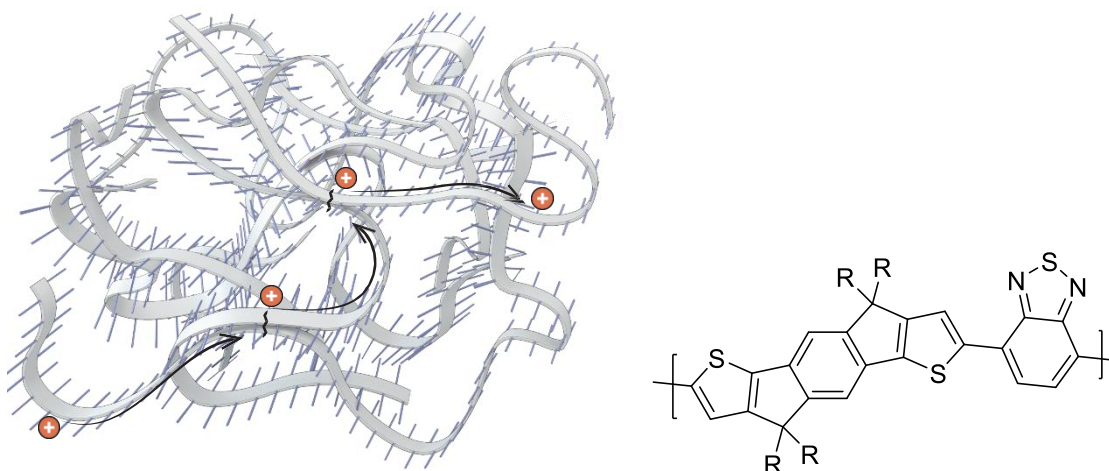174   exhibit very high charge carrier mobilities.
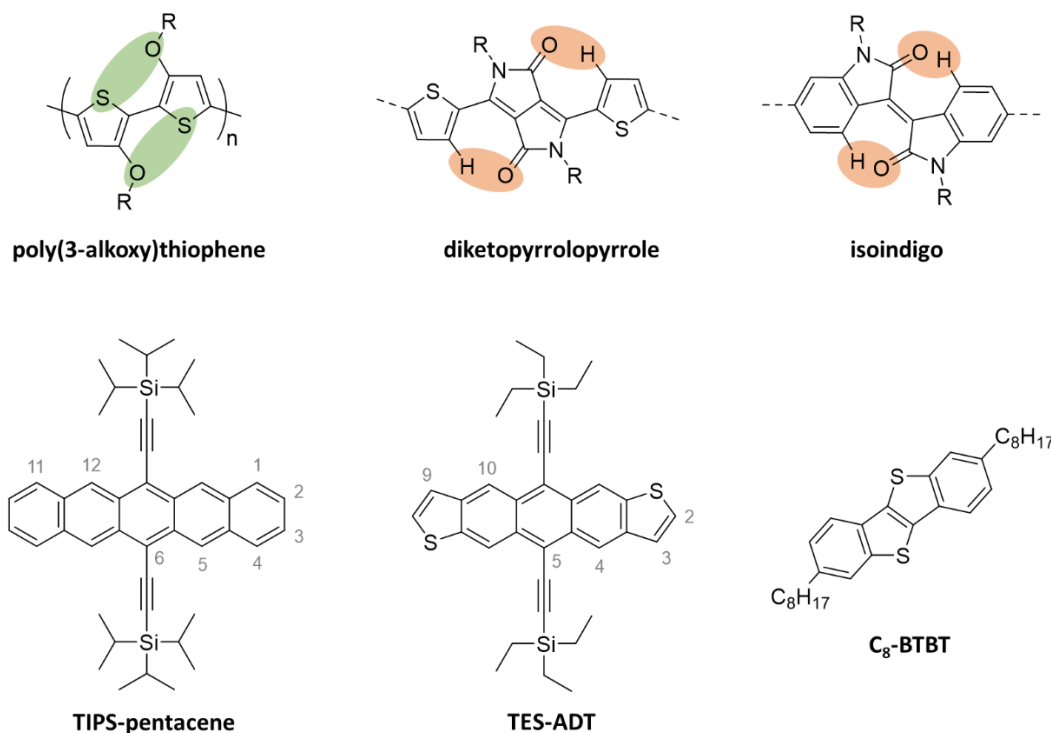
175

176

177

178

179
180

181

Figure 1. Illustration of the three-dimensional packing arrangement (left) of pBTTT , where R is typically a 14, 16 or 18 carbon linear alkyl chain and the optimal transport direction across and between domains, and (right) the intermittent short contact packing arrangement of IDT-BT where R is typically a 16 carbon linear alkyl chain   and the optimal transport direction along the chains.

Small molecule semiconductor thin film transport properties have been notoriously difficult to optimise through rational design at the molecular level. Crystal packing motifs, which are extremely sensitive to even the smallest molecular perturbations, play a dominant role, with both a herringbone and 2D slip stack arrangement being shown to have the required combination of electronic coupling and sufficient isotropy for charge propagation. Two key building blocks have emerged as exemplary aromatic cores, namely pentacene (and its analogue anthradithiophene (ADT)) and benzothienobenzothiophene (BTBT). The packing motifs of these semiconducting molecules have been manipulated by the addition of specific groups either on the central core (in the case of pentacene and ADT) or periphery (in the case of BTBT). Both pentacene and ADT can be readily centrally functionalised, on the 6 and 13 positions of the ring for pentacene [16] (most successfully with the triisopropylsilylethynyl (TIPS) group), and on the 5 and 11 positions for ADT (with triethylsilylethynyl (TES)). (Figure 1) This functionalisation serves three principal functions. It renders the molecules soluble for solution processing. It suppresses a potential oxidation site for degradation. However, most importantly, it acts as a contributing molecular template to promote a 2D

interdigitated π-stack packing motif which dramatically enhances thin film charge carrier mobilities in comparison to most other packing motifs. In contrast, replacing the isopropyl groups on the silicon atom with slightly less bulky ethyl groups (TES pentacene) dramatically changes the crystal structure, templating a lamellar 1D slip stack with a correspondingly much larger anisotropy of charge transport, which in the length-scale of a transistor device, leads to much lower charge carrier mobilities. In the case of TES-ADT, the inclusion of a peripheral fluorine atom can also promote non-covalent short contacts, further enhancing electronic coupling and subsequently carrier mobility. BTBT was identified as a suitable aromatic core for charge transport and has been most optimally substituted in the 2 and 7 positions with linear octyl chains [17]. This both increases solubility, but critically, with a highly calamitic shape, induces a herringbone packing motif. The short contacts between the conjugated cores of adjacent molecules in the crystal cell give rise to excellent, and relatively isotropic, electronic coupling, thus enhancing charge carrier mobility. Historically, the charge carrier mobility of small molecules has been larger than polymers in thin films, typically attributed to a lower energetic disorder, narrower density of states, and less defects. However, semiconducting polymers with short intermolecular contacts are catching up, and generally exhibit less anisotropy of charge transport, a feature essential for integrated circuitry.
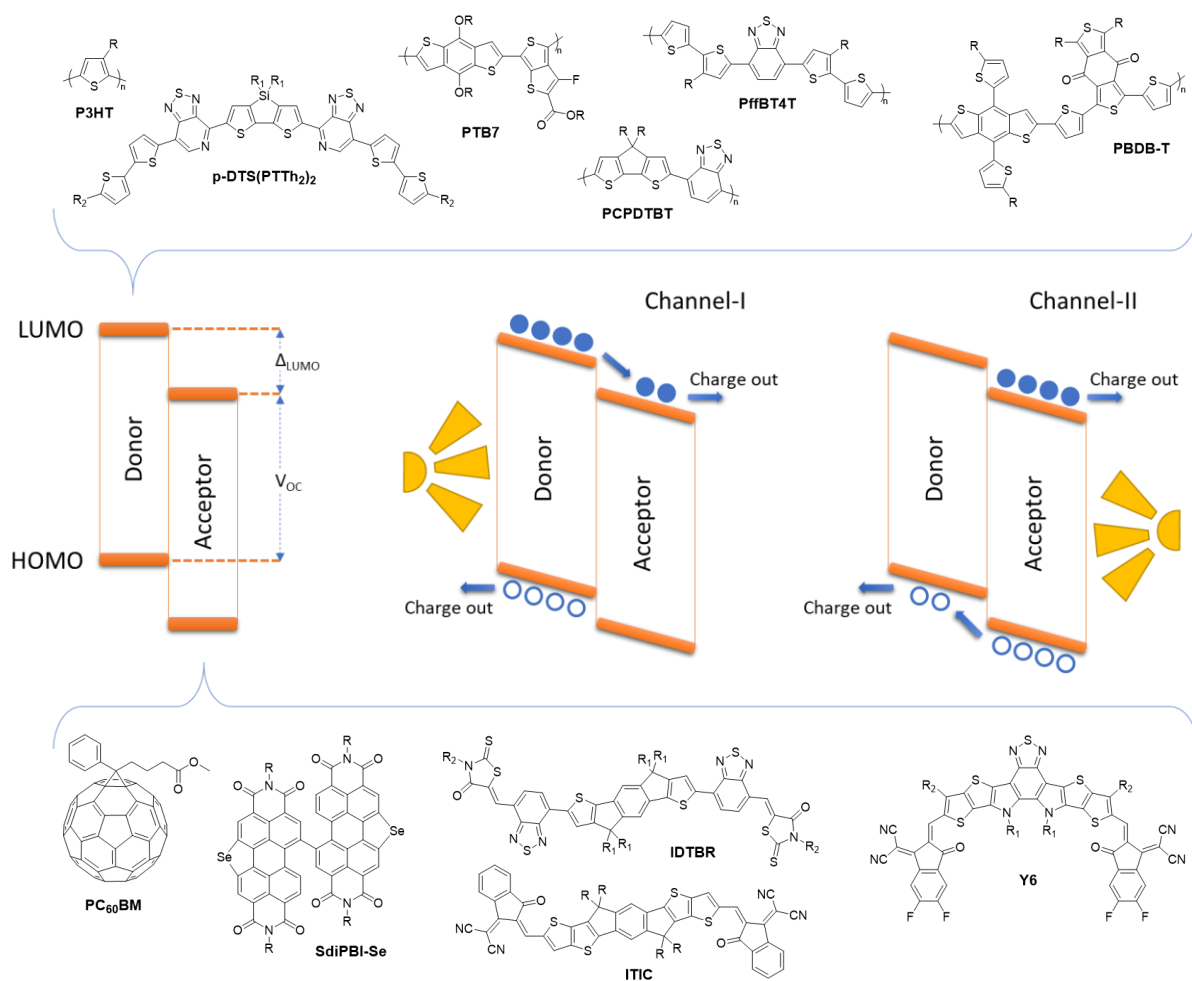

Figure 2. (top) Chemical structures of poly(3-alkoxy)thiophene , diketopyrrolopyrrole and isoindigo, with attractive planarizing interactions highlighted in green and orange. (bottom) chemical structures of highperfroming molecular semiconductors TIPS-pentacene, TES-ADT and C_8-BTBT.

Organic Photovoltaics

In an OPV device, the photoactive layer consists of an electron donor and an electron acceptor material which can both be molecularly tailored to absorb a large proportion of the incoming solar spectrum. An appropriate energetic offset between the donor and acceptor subsequently drives the splitting of excitons to free charge carriers which can be collected at the electrodes. To absorb a large proportion of the incident photons, an active layer significantly thicker than the exciton diffusion

228 length is required and this necessitates an intermixed donor:acceptor bulk heterojunction morphology
229 (BHJ).[18-20] Optimisation of the frontier molecular energy levels of both donor and acceptor such that
230 the majority of incident light is absorbed, whilst retaining sufficient energetic driving force for charge
231 separation and a high open circuit voltage (V_{oc}) is required. Additionally, the donor:acceptor
232 heterojunction must be controlled judiciously throughout the active layer to ensure efficient charge
233 separation and collection with a high degree of morphological stability.

234 In the extensively studied P3HT:PCBM heterojunction the LUMO energy levels are ~-3.2 and -4.2 eV
235 for P3HT and PCBM respectively, providing a large energetic offset to overcome the P3HT exciton
236 binding energy (typically 0.3 eV) and drive charge separation following a Channel-I mechanism
237 illustrated in Figure 3. Combined with the fact that P3HT absorbs strongly in the visible spectrum and
238 that the donor:acceptor BHJ comprises a favourable intermixed morphology, OPV devices with power
239 conversion efficiencies over 4% have been achieved.[21]

240

241 Figure 3. Energy diagrams (middle) outlining donor-acceptor energy alignment and photocurrent
242 generation, with evolution of donor (top) and acceptor (bottom) materials design.

243 In order to harvest a greater proportion of the solar spectrum, OPV research rapidly shifted from P3HT
244 towards molecular orbital hybridised donor materials by conjugating electron rich and electron poor
245 repeat units. This powerful and highly modular tool to narrow the HOMO-LUMO gap has enabled the
246 development of vast numbers of "push-pull" type polymers with hybridised molecular orbitals. While
247 a narrower band gap donor material will absorb a greater proportion of the incoming photons and
248 thus increase the extracted current (J_{sc}), it can compromise either the V_{oc} (shallower donor HOMO

249 leading to smaller LUMO(acceptor)-HOMO(donor) gap) or the charge separation (deeper donor LUMO
250 leading to smaller LUMO(donor)-LUMO(acceptor) offset) according to the energy diagram in Figure 3.
251 Computational modelling suggests that this competition between a high voltage and efficient light
252 absorption is best negotiated in a $PC_{60}BM$-based device using a donor material with a band gap around
253 1.5 eV.[22,23] One such material is PCPDTBT; despite having a near ideal band gap, it performed poorly
254 in bulk heterojunction devices. However, in 2007, the efficiency of a PCPDTBT:$PC_{70}BM$ device was
255 nearly doubled from 2.8 to 5.5% using a small amount of molecular additive (1,8-octanedithiol) when
256 casting the active layer.[24] Being able to optimise the bulk heterojunction morphology in this manner,
257 by preferentially improving the solubility of one of the photoactive components during film casting,
258 has subsequently allowed the field to more reliably assess new photoactive materials without
259 performance being overshadowed by poor morphology. Focusing still on push-pull type narrow band
260 gap donor polymers in conjunction with fullerene-based acceptors, OPV device efficiencies increased
261 steadily to around 11%, often exploiting the non-covalent interactions discussed earlier, to promote
262 polymer aggregation and facilitate phase separation at the exciton diffusion lengthscale.[25] From a
263 frontier energy level perspective, the HOMO level of these polymers, such as PTB7 (-5.15 eV), PTB7-
264 Th (-5.24 eV) and PffBT4T (-5.34 eV), have been lowered to improve the V_{oc}, while the band gap has
265 been increased slightly to ~1.6 eV. It should be noted that most high-performing PCBM devices are
266 prepared with $PC_{70}BM$; its asymmetry allows it to absorb visible light more strongly than $PC_{60}BM$, thus
267 allowing also for more Channel-II photocurrent generation (Figure 3).[26]

268 Polymer donors have dominated the OPV landscape, but there are nevertheless some notable small
269 molecule donors. The pyridalthiadiazole-based small molecule p-DTS(PTTh$_2$)$_2$ (Figure 3) with frontier
270 energy levels of -3.6 eV (LUMO) and -5.2 eV (HOMO) absorbs broadly from 500 to 800 nm and has a
271 large LUMO-LUMO offset when paired with $PC_{70}BM$.[27] Controlling the blend morphology in a two
272 molecule blend is particularly challenging, which is highlighted by a remarkable sensitivity to
273 processing conditions for the p-DTS(PTTh$_2$)$_2$:$PC_{70}BM$ devices; for a 70:30 weight ratio blend with 0.25%
274 solvent additive, a power conversion efficiency of 6.7% is achieved while small deviations from these
275 conditions sees the performance drop precipitously.

276 The V_{oc} loss is significant for Channel-I dominated fullerene-based OPV devices; defined as the
277 difference between the optical energy gap and the obtained open-circuit voltage, V_{oc} losses in high-
278 performing PCBM cells are typically on the order of 0.8 eV and thus significantly larger than the exciton
279 binding energy.[28] The development of non-fullerene acceptors (NFAs) have proven to address this
280 crucial barrier for further improving OPV device efficiencies. While it is relatively straightforward from
281 a molecular energy level perspective to design and synthesise NFAs with appropriate HOMO and
282 LUMO energy levels, early work highlighted the difficulties achieving both an intermixed blend
283 morphology and sufficiently high charge carrier mobilities. The high crystallinity of rylene diimides has
284 most successfully been mitigated by twisted dimer-type acceptor structures, for example illustrated
285 by the selenium-annulated PDI motif used in SdiPBI-Se to afford a PCE of 8.4%, and four-ring propeller-
286 type structures such as FTTB-PDI4 giving rise to a high PCE of 10.6% with a low V_{oc} loss of 0.53 V.[29,30]
287 These examples also illustrate the advantage of NFAs over fullerenes in terms of controlling the
288 frontier energy levels with relative ease; SdiPBI-Se and FTTB-PDI4 have LUMO energy levels of -3.9
289 and -3.6 eV and optical band gaps of 2.2 and 1.9 eV, respectively. Not only can the acceptor strength
290 be adjusted to match the chosen donor material, the optical band gap can likewise be tuned to ensure
291 complementary absorption with the donor. The control over frontier energy levels is further
292 emphasised by the fact that NFAs often have their HOMOs and LUMOs spatially separated meaning
293 that they can be adjusted independently of each other through molecular design (see tutorial box for
294 more detail). Additionally, NFAs typically show markedly enhanced light absorption compared to

295 fullerene acceptors; coupled with efficient hole transfer from acceptor to donor, this provides high
296 Channel-II photocurrent generation and high J_{sc} values.

297 A further leap for NFAs has been manifested through the recent development of calamitic π-
298 conjugated molecules characterised by a central fused electron-rich (hetero)aromatic core flanked by
299 terminal electron-deficient units such as indanedione or rhodanine; further modularity in the
300 molecular design can be incorporated by inserting electron-rich or deficient π-conjugated spacers
301 between the core and the flanking groups. IDTBR, with an indacenodithiophene core flanked on each
302 side by 2,1,3-benzothiadiazole and rhodanine, is one such calamitic acceptor.[31] Its co-planar backbone
303 results in a relatively narrow band gap (1.6 eV); a P3HT:IDTBR active layer consequently absorbs
304 strongly over the entire visible spectrum and affords device efficiencies above 6%. In addition to
305 pushing the OPV performance for a simple and commercially scalable polymer such as P3HT, this work
306 also illustrates that the NFAs can be used as the primary low band gap light absorber, a role which was
307 hitherto reserved for the donor material. Further improvements towards 8% power conversion
308 efficiency with IDTBR has been reported for ternary blends using two complementary NFAs in
309 conjunction with P3HT.[32] IDTBR has a LUMO energy level of -3.9 eV, making it compatible in terms of
310 LUMO-LUMO offset with polymers such as PffBT4T; this is clearly demonstrated with a power
311 conversion efficiency of 10% and a very small V_{oc} loss around 0.5 V for a PffBT4T:IDTBR based device.[33]
312 ITIC is another calamitic acceptor with comparable frontier energy levels to those of IDTBR.[34] It has
313 likewise been used in several high efficiency OPV devices, but similarly to IDTBR it has an optical band
314 gap around 1.6 eV which is comparable to most high-performing donor polymers developed
315 specifically for fullerene-based devices. As such, to cover more of the solar spectrum and increase J_{sc},
316 it has proven beneficial to widen the band gap of the donor polymer to prevent a large spectral overlap
317 with the NFA, and possibly provide a pathway for Forster Energy transfer from the donor to acceptor.
318 PBDB-T, with a HOMO level of -5.3 eV and an optical band gap around 1.8 eV, comprises the weaker
319 acceptor unit benzodithiophenedione as the electron-deficient unit in conjunction with the well-
320 known benzodithiophene donor motif. Devices with a PBDB-T:ITIC active layer have gradually been
321 improved to over 14% device efficiency.[35,36] PBDB-T has been modified by substitution of alkyl chains
322 with thioalkyls, by fluorination and chlorination, while ITIC similarly has been fluorinated and
323 chlorinated. Halogenation of the ITIC electron acceptor increases its electron withdrawing potential,
324 and stabilises both the HOMO and LUMO, but more so the LUMO, as there is a higher LUMO orbital
325 distribution on the ITIC unit, which results in a slightly narrower band gap. The red-shifted absorption
326 increases the J_{sc} while enhanced intra- and intermolecular interactions concurrently improve the
327 extinction coefficient and charge transport properties. The HOMO energy level of dichlorinated PBDB-
328 T-2Cl is lowered 0.2 eV relative to its non-chlorinated analogue PBDB-T; this maintains a high V_{oc} in
329 OPV devices with halogenated ITIC derivatives, while the stabilised frontier energy levels likewise
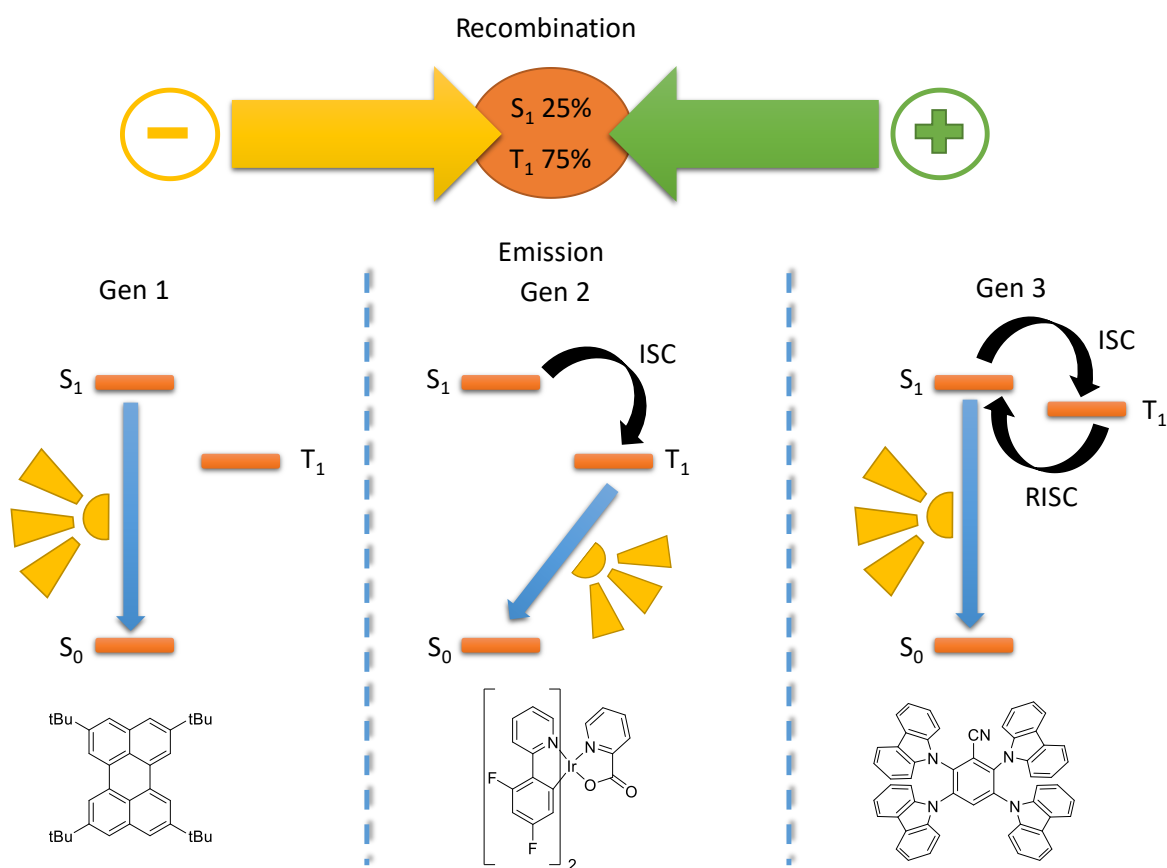330 improve the device oxidative stability.

331 Most recently, attention has broadened from linear calamitic motifs to a curved structure in the form
332 of Y6.[37] Introducing as the central π-conjugated chromophore a 2,1,3-benzothiadiazole flanked by
333 thieno[3,2-*b*]thiophene units that are fused onto the benzothiadiazole with alkyl-bearing nitrogen
334 atoms, a narrow band gap NFA absorbing strongly beyond 900 nm is obtained. The two *N*-alkyl side
335 chains facing each other in Y6 twist the molecule slightly (~17 degrees), ensuring good solubility and
336 favourable control of aggregation. Paired with a fluorinated derivative of PBDB-T devices obtained
337 high power conversion efficiencies above 15% with V_{oc} values above 0.8 V. The small V_{oc} loss for this
338 system is further improved using a chlorinated analogue of Y6, giving a device efficiency above 16%
339 and a V_{oc} loss of only 0.53 V with a small non-radiative energy loss of 0.2 V.[38] It is hypothesised that
340 the much larger dipole moments in these bent NFAs compared to ITIC-type NFAs, and high electron
341 mobility, contribute to the efficient charge separation and high fill factors around 75%.

342 While it is clear that molecule structure and frontier energy level design has driven the field of OPV
343 forward continuously over the last decade, related design approaches are likewise being explored to
344 sensitise other PV applications. This is most prominently exemplified with the development of singlet
345 fission materials that convert one high-energy singlet exciton to two lower energy triplet excitons,
346 which can in turn generate additional electron-hole pairs in, for example, low bandgap silicon-based
347 PV devices. With an S_1 singlet exciton energy of 2.4 eV, tetracene can absorb high-energy photons that
348 would otherwise generate high thermalisation losses in silicon cells and subsequently through the
349 process of singlet fission convert this singlet exciton to two triplet excitons. The T_1 triplet exciton
350 energy of tetracene around 1.25 eV matches nicely the 1.1 eV bandgap of silicon. Although it is proving
351 challenging to effectively transfer the triplet excitons to the silicon cell, this technology holds promise
352 to exceed the Shockley-Queisser limit of 29% efficiency for a single junction PV device.

353

354 **Organic Light Emitting Diodes**

355 Despite organic light emitting diodes (OLEDs) being at an advanced stage of commercialisation, it
356 remains an extremely active area of research with many fascinating developments over the last 5-10
357 years. The fundamental operating principle of an OLED is extremely simple; charges injected from
358 electrodes recombine within an organic layer to form an excited state which decays radiatively.
359 However, spin statistics dictates that non-geminate recombination of charges results in a 1:3 ratio of
360 singlet and triplet excited states. The vast majority of research since the birth of the OLED has been to
361 overcome the issue associated with the non-emissive nature of triplet excited states which limits a
362 maximum of 25% internal quantum efficiency (IQE). The first successful approach to overcome this
363 was to move away from fluorescence (Gen 1) to phosphorescence (Gen 2) by exploiting the efficient
364 heavy-metal induced intersystem crossing and phosphorescence of organo-platinum and iridium
365 complexes (Figure 4). This allowed all of the electrically generated excited states to be used radiatively
366 and 100% internal quantum efficiency devices were demonstrated (with a maximum of 20-25%
367 external quantum efficiency due to outcoupling losses). However, issues associated with both colour
368 purity, and stability particularly in the blue region of the electromagnetic spectrum motivated
369 researchers to continue developing new materials for OLEDs. The 3rd generation of OLED materials
370 relies on the principle of reverse intersystem crossing (rISC) to utilise the dark triplet states. By
371 reducing the energy gap between the lowest excited singlet and triplet states, rISC can take place
372 whereby triplets can be converted into emissive singlets using thermal energy, i.e. thermally activated
373 delayed fluorescence (TADF).

Figure 4: Evolution of OLED Emitters

The most commonly used phosphorescent emitters are cyclometallated iridium (III) complexes which are dispersed within an organic host. It has long been known that the emitting dipole orientation of a dye influences the outcoupling efficiency of OLEDs.[39] Despite this, the dipole orientation of phosphoresecent dopants has not been studied extensively, presumably due to the lack of any obvious driving force for alignment (in typically amorphous host materials). It has recently been shown using angle-dependent polarized photoluminescent emission spectroscopy that certain iridium complexes can be aligned in films.[40,41] They suggested that the inherent asymmetry at the surface of a growing film promotes dopant alignment in these otherwise amorphous films. Alongside other investigations to investigate and control phosphor alignment, external quantum efficiencies in excess of 30% have been reported with projected efficiencies of up to 60% believed possible.[39,42] Despite decades of research, new strategies for achieving efficient blue emission from Iridium complexes are still being sought with very impressive results being demonstrated recently. Isomerisation of a UV emitting N-heterocyclic carbene based Ir(III) complex from *fac* to *mer* subtly red-shifted its emission such that it displayed efficient deep blue phosphorescence with ~80% PLQY and EQE ~ 15%.[43] There have also been considerable progress in the development non-iridium based phosphorescent emitters. Recently, a new class of cyclometalated Au(III) complexes with tuneable emission spanning sky-blue to red were reported. These materials exhibited high photoluminescence quantum yields (PLQY) of up to 80% in solid-state thin films and impressive performance in OLEDs with EQEs up to 22% reported with excellent stability.[37] An extremely active area of research is the development of near-IR OLED emitters for security and communication applications. A new class of Pt(II) complexes that emit light at 740 nm with a PLQY of 81% were recently reported In conjugation with a highly preferred horizontal dipole orientation OLED devices exhibited an external quantum efficiency of 24 %.[44] The origin of the near-IR emission was attributed to the stacking of Pt(II) complexes in the solid state.

399 Almost certainly the biggest development in the field of OLEDs over the last 10 years has been the
400 demonstration of TADF using purely organic dyes. This work was pioneered by the group of Adachi
401 with the seminal publication demonstrating a series of purely organic materials with high PLQY
402 tuneable emission and OLED EQEs approaching 20%.[45] Within this work was detailed the simple design
403 concept that by spatially separating a molecule's HOMO and LUMO through a twisted donor-acceptor
404 structure, the energy gap between the first excited singlet and triplet could be substantially reduced.
405 This allows triplet states to be converted into emissive singlets through reverse intersystem crossing
406 (rISC) resulting in the phenomenon of thermally activated delayed fluorescence. By tuning the number,
407 twist and electron density of donors to acceptors, extremely impressive PLQY and OLED EQEs have
408 been obtained spanning blue to near-IR.[46,47,48,49,50] Despite these extremely impressive results, the
409 exact mechanism by which rISC and TADF occur remains the subject of debate. It was rapidly
410 established that in order to design efficient TADF emitters it is vital to consider both locally excited
411 (LE) and charge-transfer (CT) states.[51] However, the process by which the spin-flip between singlet and
412 triplet states is not clear. It has been suggested that 'hidden' n-pi mixed states may play an important
413 role in the process or that second order vibronic coupling between the various excited states is
414 required.[52-54] Very recently, the important role of intermediate electronic states that mediate the spin-
415 flip process through molecular vibrations has been demonstrated using a new model which also
416 complements the notion of non-adiabatic coupling of triplet states promoting ISC.[55] Therefore, the
417 synthetic strategy of merely minimising the S_1-T_1 energy gap requires refinement. One of the issues
418 with conventional TADF is the requirement of highly twisted D-A structures, which results in broad
419 spectral emission with low oscillator strength. This can potentially be overcome using a
420 "hyperfluoresence" strategy whereby a fluorescent guest is introduced into a TADF host albeit at the
421 expense of device simplicity.[56] It has also been suggested that using a 'multi-resonant' strategy, which
422 spatially separates HOMO and LUMO within a single planar molecule, narrow ΔE_{ST} gap materials with
423 high oscillator strength and narrow emission can be obtained.[57,58] Indeed, extremely impressive
424 results using this strategy has recently been reported with a blue (469 nm) organoboron TADF emitter
425 based OLED with an EQE of 34%.[59]

426 TADF has also been observed in organometallic systems, with Cu(I)-Carbene complexes demonstrating
427 outstanding optoelectronics properties in particular. Photoluminescence quantum yields of 100%
428 have been reported and OLED device efficiencies of >25% EQE.[60,61] Emission in these systems appears
429 to stem from inter-ligand charge transfer states and importantly it appears that (as has also been
430 suggested in organic TADF[62]) that there is considerable spin-mixing occurring, further indicating that
431 the "spin-pure" picture of TADF emitters may be overly simplistic. However, similarly to
432 phosphoresecent OLED emitters, achieving highly stable blue OLEDs with good colour purity have
433 proved extremely challenging.

434

435 **Beyond the state of the art**

436 A typical chemical design approach for semiconductor optimisation involves systematic variations in
437 the aromatic conjugated units comprising the core or backbone, undertaken in order to isolate and
438 study the molecular design effect on both morphology and frontier molecular orbital energy levels. As
439 a justification of the design concept, results are often compared with previous publications. In the
440 transistor field, unreliable charge carrier mobility values, extracted from invalid model equations and
441 assumptions, has both inflated expectations and led to incorrect structure-property relationships
442 being proposed, with molecular design conclusions reached on tenuous evaluations. This has seriously
443 impeded progress in new materials for transistor applications. However, there are clearly some

444 obvious opportunities for further exploration. The presence of aliphatic chains in these materials is
445 primarily to impart solubility and secondarily control solid-state structure. However, both alkyl chain
446 and lamellar crystallisation can come at the *expense* of conjugated backbone planarity and crystallinity.
447 It is imperative that new semiconductor design is done in a holistic fashion whereby the self-assembly
448 of the system works with, rather than against optimum performance. It may be possible to utilise side
449 chains in creative new ways such as the suppression of various undesirable phonon modes which have
450 recently been shown to severely affect charge transport.[63] Alternatively, entirely removing the alky
451 chains should fundamentally improve charge transport. In-situ side chain detachment methods to
452 increase backbone densification, without compromising microstructural order is a promising approach
453 to performance improvement, yet currently most methods remove the inert chains at the expense of
454 order and percolation, thus reducing transport properties. Molecular order however has proven to be
455 key in optimising charge transport and finding ways to further reduce the disorder in conjugated
456 systems or alternatively design materials with a higher tolerance towards rotational fluctuations, will
457 be essential to improve the charge transport further. To date this approach has proven challenging as
458 it is difficult to predict solid state packing of organic semiconductors and the different vibrational
459 modes associated with a particular unit cell. With improving computational capabilities however
460 material property predictions are getting ever more sophisticated and accurate, providing important
461 insight into material packing motifs and phonon coupling modes. This opens up the opportunity to not
462 only calculate the many phonon coupling modes in a conjugated system, but most importantly to
463 predict and identify the modes most detrimental to charge carrier transport.

464 Besides the electronic charge transport, mixed conduction, i.e. the ability of organic conductors and
465 semiconductors to facilitate both electronic and ionic charge transport in the solid state, is achieving
466 a growing amount of attention due to potential use for biological interfacing.[64,65] In this context, the
467 organic electrochemical transistor (OECT), a three-terminal device that can be gated through an
468 aqueous electrolyte, is emerging as a powerful tool for bioelectronic applications. In an OECT, the bulk
469 active layer contributes to the current modulation through doping or dedoping. Development of n-
470 and p-type semiconducting polymers for OECTs therefore necessitate new design rules for frontier
471 energy level optimisation. For stable operation in aqueous environments, as a first prerequisite, the
472 HOMO level of p-type materials must be electrochemically accessible before water electrolysis takes
473 place at 1.23 V (versus the normal hydrogen electrode (NHE)). High performance mixed conductors
474 have much shallower HOMO levels around -4.4 to -4.6 eV depending on the measurement
475 technique.[66,67] Shallow HOMO levels in that range are obtained with glycolated polythiophenes similar
476 to the poly(3-alkoxythiophene) depicted in Figure 1 where the oxygen atoms mesomerically donate
477 electron density to the polymer backbone while the polar nature of the oligoether sidechain facilitates
478 ion transport. The development of n-type semiconductors is essential for sensing of biologically
479 relevant metabolites and cations, such as sodium, potassium and calcium. To be operationally stable
480 in water, the main challenge centres around the stability of the radical anions towards water and/or
481 oxygen.[68] Here, LUMO levels deeper than -4.0 eV are required.[69,70] Currently the performance of
482 electron transport OECT semiconductors significantly lags behind their hole transporting counterparts.
483 Although this has been tentatively attributed to coulombic charge pinning from counterions, charge
484 trapping from water, and other phenomena, new molecular designs are required to overcome these
485 limitations.

486 For photovoltaic applications on the other hand, the focus should not be on optimising the electronic
487 and solid state properties of a single material, but rather on understanding the design criteria to
488 control the morphology of the active layer, perhaps incorporating multiple materials, chosen to create
489 an energy cascade with large charge transfer (CT) state energies. While the frontier energy levels and
490 the isolated molecular packing of both donor and acceptor is generally well controlled, morphological

491 control through molecular design is still lacking, both on microscopic and macroscopic length scales.
492 Although morphological stability of the BHJ blend has been improved significantly by the introduction
493 of low diffusive NFAs, it would be highly advantageous if the tertiary structure could be controlled to
494 a greater extent for instance by choice of heteroatoms, functional groups and sidechains. Ideally, such
495 approaches should also provide a means to firstly generate much thicker photoactive layers without
496 unwanted vertical phase separation and excessive charge recombination and secondly scale up the
497 cell's active area more effortlessly. At much shorter length scales, being able to control the donor-
498 acceptor interfaces in the blend, for instance through molecular shape and dipole moments, would
499 allow for greater understanding and control of the energy and charge transfer processes. Another
500 important aspect that require further attention is the role of the CT state, how the CT state can be
501 manipulated through chemical design and how this can be utilised to suppress recombination
502 processes. Recent work indicates that electrostatic potential mapping for instance could be a useful
503 tool to help understand how molecular structure and intermolecular interactions influence the charge
504 separation processes.[71] The recent reports of Y6, a curved NFA structure markedly different from the
505 previous best NFA performers in terms of molecular design, has to a large extent taken the OPV
506 community by surprise. While it promisingly shows that there is still ample room for device
507 performance improvements, it also underlines that a unified picture on molecular design criteria has
508 not yet been developed. The understanding of NFAs, their detailed structure-property relations and
509 the dominating reasons for the excellent performance continue to be explored. Factors such as off-
510 axis dipole, high electron mobility, facile energy transfer processes and the potential for good Forster
511 energy overlap with the donor could potentially play significant roles. As the community now embarks
512 on in-depth fundamental studies of Y6-based devices as well as the synthesis of Y6 analogues, further
513 pieces of this puzzle will emerge, which in turn will push the device performance closer towards the
514 20% efficiency mark and hopefully add to the understanding of molecular and frontier energy level
515 design criteria.

516 The commercialisation of OLED technology has already been a monumental success. However, a
517 detailed understanding of the exact photophysical processes occurring during charge recombination
518 and emission is required alongside a clear relationship between chemical structure and photophysical
519 properties for continuing progress to be achieved. It is clearly necessary to further understand the
520 origin of stability/instability of excited states in particular in the presence of charges. Identification of
521 degradation pathways may allow suitable chemical modification to prevent the degradation of these
522 materials. Despite this, current generations of OLED materials are operating close to their theoretical
523 maxima and for a step-change in performance, a new generation of materials must be developed.
524 Some encouraging signs of emerging 4th generation, which warrant exploration, are as follows. There
525 have been recent reports of extremely efficient OLED devices using radical based fluorophores.[72,73]
526 These compounds, based on the well-known luminescent tris(2,4,6-trichlorophenyl)methyl (TTM)
527 radical emit from a doublet excited state entirely circumventing spin dependent recombination.
528 However, thus far these materials have only demonstrated electroluminescence in the red/near-IR
529 and it remains to be seen whether it is possible to tune them to cover the entire visible spectrum.
530 Another interesting new approach by Adachi *et al.* involves the use of host materials capable of
531 undergoing singlet fission which, in principle, could allow for IQEs of 200%.[74] Very low EQEs for this
532 device were observed due to the low PLQY of the emitting guest erbium (III) complex. In order for this
533 strategy to succeed it will be necessary to develop wide band-gap singlet fission hosts and/or highly
534 emissive near-IR emitters capable of harvesting triplet excitons. There have been several recent
535 reports of utilising triplet fusion for OLEDs whereby two triplets annihilate and produce an emissive
536 singlet.[75-77] Although this limits IQE to a maximum of 50% (if only triplets are injected) it could
537 potentially allow for low driving voltages and may offer stability advantages for blue emitters.

538 There is also a need to improve the underpinning chemistry used to synthesise organic
539 semiconductors. The presence of (often hard to detect) residual impurities can result in batch-to-batch
540 variations or unintentional doping. The availability and compatibility of chemical building blocks
541 dictates the choice of chemistry employed in synthesis. Polymerisations often relies on palladium
542 catalysed cross-coupling methodology (i.e. Yamamoto, Suzuki, and particularly Stille) and while these
543 coupling reactions are extremely efficient, their atom economy and use of chlorinated solvents does
544 not comply with sustainability requirements, nor are they particularly suitable for large scale
545 production. C-H activation and condensation chemistry circumvents some of these problems, by
546 shortening the synthetic pathway and making the extensive functionalisation of the monomers
547 obsolete.[78] The narrow scope and imposed restrictions on employable building blocks however leave
548 amble room for improvement. Developing new chemical polymerisation protocols that allow for
549 control over molecular weight and polydispersity whilst reducing chemical defects (i.e. homocoupling,
550 partial oxidation) will be an integral part in advancing the quality of the synthesised materials.

551

552

553 **Uncategorized References**

554 1   Holliday, S. *et al.* A Rhodanine Flanked Nonfullerene Acceptor for Solution-Processed
555   Organic Photovoltaics. *Journal of the American Chemical Society* **137**, 898-904,
556   doi:10.1021/ja5110602 (2015).
557 2   Planells, M., Schroeder, B. C. & McCulloch, I. Effect of Chalcogen Atom Substitution on the
558   Optoelectronic Properties in Cyclopentadithiophene Polymers. *Macromolecules* **47**, 5889-
559   5894, doi:10.1021/ma5014308 (2014).
560 3   Nikolka, M. *et al.* High operational and environmental stability of high-mobility conjugated
561   polymer field-effect transistors through the use of molecular additives. *Nature Materials* **16**,
562   356, doi:10.1038/nmat4785

563 https://www.nature.com/articles/nmat4785#supplementary-information (2016).
564 4   de Leeuw, D. M., Simenon, M. M. J., Brown, A. R. & Einerhand, R. E. F. Stability of n-type
565   doped conducting polymers and consequences for polymeric microelectronic devices. *Synth.*
566   *Met.* **87**, 53-59 (1997).
567 5   Abbaszadeh, D. *et al.* Electron trapping in conjugated polymers. *Chemistry of Materials*,
568   doi:10.1021/acs.chemmater.9b01211 (2019).
569 6   Usta, H. *et al.* Design, Synthesis, and Characterization of Ladder-Type Molecules and
570   Polymers. Air-Stable, Solution-Processable n-Channel and Ambipolar Semiconductors for
571   Thin-Film Transistors via Experiment and Theory. *Journal of the American Chemical Society*
572   **131**, 5586-5608, doi:10.1021/ja809555c (2009).
573 7   McCulloch, I. *et al.* Liquid-crystalline semiconducting polymers with high charge-carrier
574   mobility. *Nat. Mater.* **5**, 328-333, doi:10.1038/nmat1612 (2006).
575 8   Lei, T. *et al.* Systematic Investigation of Isoindigo-Based Polymeric Field-Effect Transistors:
576   Design Strategy and Impact of Polymer Symmetry and Backbone Curvature. *Chemistry of*
577   *Materials* **24**, 1762-1770, doi:10.1021/cm300117x (2012).
578 9   Venkateshvaran, D. *et al.* Approaching disorder-free transport in high-mobility conjugated
579   polymers. *Nature* **515**, 384-388, doi:10.1038/nature13854 (2014).
580 10   Lemaur, V. *et al.* Resilience to conformational fluctuations controls energetic disorder in
581   conjugated polymer materials: Insights from atomistic simulations. *Chemistry of Materials*,
582   doi:10.1021/acs.chemmater.9b01286 (2019).
583 11   Nielsen, C. B., White, A. J. P. & McCulloch, I. Effect of Fluorination of 2,1,3-Benzothiadiazole.
584   *The Journal of Organic Chemistry* **80**, 5045-5048, doi:10.1021/acs.joc.5b00430 (2015).

585   12   Conboy, G. *et al.* To bend or not to bend – are heteroatom interactions within conjugated
586   molecules effective in dictating conformation and planarity? *Materials Horizons* **3**, 333-339,
587   doi:10.1039/C6MH00051G (2016).
588   13   Thorley, K. J. & McCulloch, I. Why are S–F and S–O non-covalent interactions stabilising?
589   *Journal of Materials Chemistry C* **6**, 12413-12421, doi:10.1039/C8TC04252G (2018).
590   14   von, H. Structure cristalline de l'isoindigo. *Acta Crystallographica* **13**, 936-938,
591   doi:doi:10.1107/S0365110X60002272 (1960).
592   15   Naik, M. A., Venkatramaiah, N., Kanimozhi, C. & Patil, S. Influence of Side-Chain on Structural
593   Order and Photophysical Properties in Thiophene Based Diketopyrrolopyrroles: A Systematic
594   Study. *The Journal of Physical Chemistry C* **116**, 26128-26137, doi:10.1021/jp306365q (2012).
595   16   Anthony, J. E., Brooks, J. S., Eaton, D. L. & Parkin, S. R. Functionalized Pentacene: Improved
596   Electronic Properties from Control of Solid-State Order. *Journal of the American Chemical*
597   *Society* **123**, 9482-9483, doi:10.1021/ja0162459 (2001).
598   17   Ebata, H. *et al.* Highly Soluble [1]Benzothieno[3,2-b]benzothiophene (BTBT) Derivatives for
599   High-Performance, Solution-Processed Organic Field-Effect Transistors. *Journal of the*
600   *American Chemical Society* **129**, 15732-15733, doi:10.1021/ja074841i (2007).
601   18   Sariciftci, N. S., Smilowitz, L., Heeger, A. J. & Wudl, F. Photoinduced electron transfer from a
602   conducting polymer to buckminsterfullerene. *Science* **258**, 1474-1476,
603   doi:10.1126/science.258.5087.1474 (1992).
604   19   Yu, G., Gao, J., Hummelen, J. C., Wudl, F. & Heeger, A. J. Polymer Photovoltaic Cells:
605   Enhanced Efficiencies via a Network of Internal Donor-Acceptor Heterojunctions. *Science*
606   **270**, 1789-1791, doi:10.1126/science.270.5243.1789 (1995).
607   20   Tamai, Y., Ohkita, H., Benten, H. & Ito, S. Exciton Diffusion in Conjugated Polymers: From
608   Fundamental Understanding to Improvement in Photovoltaic Conversion Efficiency. *J Phys*
609   *Chem Lett* **6**, 3417-3428, doi:10.1021/acs.jpclett.5b01147 (2015).
610   21   Kim, Y. *et al.* A strong regioregularity effect in self-organizing conjugated polymer films and
611   high-efficiency polythiophene:fullerene solar cells. *Nature Materials* **5**, 197-203,
612   doi:10.1038/nmat1574 (2006).
613   22   Scharber, M. C. *et al.* Design Rules for Donors in Bulk-Heterojunction Solar Cells—Towards
614   10 % Energy-Conversion Efficiency. *Advanced Materials* **18**, 789-794,
615   doi:10.1002/adma.200501717 (2006).
616   23   Kirkpatrick, J. *et al.* A Systematic Approach to the Design Optimization of Light-Absorbing
617   Indenofluorene Polymers for Organic Photovoltaics. *Advanced Energy Materials* **2**, 260-265,
618   doi:10.1002/aenm.201100622 (2012).
619   24   Peet, J. *et al.* Efficiency enhancement in low-bandgap polymer solar cells by processing with
620   alkane dithiols. *Nat Mater* **6**, 497-500, doi:10.1038/nmat1928 (2007).
621   25   Liu, Y. *et al.* Aggregation and morphology control enables multiple cases of high-efficiency
622   polymer solar cells. *Nature Communications* **5**, 5293, doi:10.1038/ncomms6293

623   https://www.nature.com/articles/ncomms6293#supplementary-information (2014).
624   26   Dimitrov, S. D. *et al.* Towards optimisation of photocurrent from fullerene excitons in organic
625   solar cells. *Energy & Environmental Science* **7**, 1037, doi:10.1039/c3ee42607f (2014).
626   27   Sun, Y. *et al.* Solution-processed small-molecule solar cells with 6.7% efficiency. *Nat Mater*
627   **11**, 44-48, doi:10.1038/nmat3160 (2011).
628   28   Li, W., Hendriks, K. H., Furlan, A., Wienk, M. M. & Janssen, R. A. High quantum efficiencies in
629   polymer solar cells at energy losses below 0.6 eV. *J Am Chem Soc* **137**, 2231-2234,
630   doi:10.1021/ja5131897 (2015).
631   29   Meng, D. *et al.* High-Performance Solution-Processed Non-Fullerene Organic Solar Cells
632   Based on Selenophene-Containing Perylene Bisimide Acceptor. *J Am Chem Soc* **138**, 375-380,
633   doi:10.1021/jacs.5b11149 (2016).

634 30 Zhang, J. *et al.* Ring-Fusion of Perylene Diimide Acceptor Enabling Efficient Nonfullerene
635   Organic Solar Cells with a Small Voltage Loss. *J Am Chem Soc* **139**, 16092-16095,
636   doi:10.1021/jacs.7b09998 (2017).
637 31 Holliday, S. *et al.* High-efficiency and air-stable P3HT-based polymer solar cells with a new
638   non-fullerene acceptor. *Nature Communications* **7**, 11585, doi:10.1038/ncomms11585

639 https://www.nature.com/articles/ncomms11585#supplementary-information (2016).
640 32 Baran, D. *et al.* Reducing the efficiency-stability-cost gap of organic photovoltaics with highly
641   efficient and stable small molecule acceptor ternary solar cells. *Nat. Mater.* **16**, 363-369,
642   doi:10.1038/nmat4797 (2017).
643 33 Baran, D. *et al.* Reduced voltage losses yield 10% efficient fullerene free organic solar cells
644   with >1 V open circuit voltages. *Energy Environ Sci* **9**, 3783-3793, doi:10.1039/c6ee02598f
645   (2016).
646 34 Lin, Y. *et al.* An electron acceptor challenging fullerenes for efficient polymer solar cells. *Adv*
647   *Mater* **27**, 1170-1174, doi:10.1002/adma.201404317 (2015).
648 35 Zhao, W. *et al.* Molecular Optimization Enables over 13% Efficiency in Organic Solar Cells. *J*
649   *Am Chem Soc* **139**, 7148-7151, doi:10.1021/jacs.7b02677 (2017).
650 36 Zhang, H. *et al.* Over 14% Efficiency in Organic Solar Cells Enabled by Chlorinated
651   Nonfullerene Small-Molecule Acceptors. *Adv Mater* **30**, e1800613,
652   doi:10.1002/adma.201800613 (2018).
653 37 Yuan, J. *et al.* Single-Junction Organic Solar Cell with over 15% Efficiency Using Fused-Ring
654   Acceptor with Electron-Deficient Core. *Joule*,
655   doi:https://doi.org/10.1016/j.joule.2019.01.004 (2019).
656 38 Cui, Y. *et al.* Over 16% efficiency organic photovoltaic cells enabled by a chlorinated acceptor
657   with increased open-circuit voltages. *Nat Commun* **10**, 2515, doi:10.1038/s41467-019-
658   10351-5 (2019).
659 39 Kim, K.-H. & Kim, J.-J. Origin and Control of Orientation of Phosphorescent and TADF Dyes
660   for High-Efficiency OLEDs. *Advanced Materials* **30**, 1705600, doi:10.1002/adma.201705600
661   (2018).
662 40 Jurow, M. J. *et al.* Understanding and predicting the orientation of heteroleptic phosphors in
663   organic light-emitting materials. *Nature Materials* **15**, 85, doi:10.1038/nmat4428

664 https://www.nature.com/articles/nmat4428#supplementary-information (2015).
665 41 Schmidt, T. D. *et al.* Emitter Orientation as a Key Parameter in Organic Light-Emitting Diodes.
666   *Physical Review Applied* **8**, 037001, doi:10.1103/PhysRevApplied.8.037001 (2017).
667 42 Moon, C.-K., Kim, K.-H. & Kim, J.-J. Unraveling the orientation of phosphors doped in organic
668   semiconducting layers. *Nature Communications* **8**, 791, doi:10.1038/s41467-017-00804-0
669   (2017).
670 43 Lee, J. *et al.* Deep blue phosphorescent organic light-emitting diodes with very high
671   brightness and efficiency. *Nature Materials* **15**, 92, doi:10.1038/nmat4446

672 https://www.nature.com/articles/nmat4446#supplementary-information (2015).
673 44 Tuong Ly, K. *et al.* Near-infrared organic light-emitting diodes with very high external
674   quantum efficiency and radiance. *Nature Photonics* **11**, 63, doi:10.1038/nphoton.2016.230

675 https://www.nature.com/articles/nphoton.2016.230#supplementary-information (2016).
676 45 Uoyama, H., Goushi, K., Shizu, K., Nomura, H. & Adachi, C. Highly efficient organic light-
677   emitting diodes from delayed fluorescence. *Nature* **492**, 234, doi:10.1038/nature11687

678 https://www.nature.com/articles/nature11687#supplementary-information (2012).
679 46 Hirata, S. *et al.* Highly efficient blue electroluminescence based on thermally activated
680   delayed fluorescence. *Nature Materials* **14**, 330, doi:10.1038/nmat4154

681 https://www.nature.com/articles/nmat4154#supplementary-information (2014).

682 47   Zhang, Q. *et al.* Efficient blue organic light-emitting diodes employing thermally activated
683   delayed fluorescence. *Nature Photonics* **8**, 326, doi:10.1038/nphoton.2014.12

684   https://www.nature.com/articles/nphoton.2014.12#supplementary-information (2014).
685 48   Lin, T.-A. *et al.* Sky-Blue Organic Light Emitting Diode with 37% External Quantum Efficiency
686   Using Thermally Activated Delayed Fluorescence from Spiroacridine-Triazine Hybrid.
687   *Advanced Materials* **28**, 6976-6983, doi:10.1002/adma.201601675 (2016).
688 49   Kaji, H. *et al.* Purely organic electroluminescent material realizing 100% conversion from
689   electricity to light. *Nature Communications* **6**, 8476, doi:10.1038/ncomms9476

690   https://www.nature.com/articles/ncomms9476#supplementary-information (2015).
691 50   Zeng, W. *et al.* Realizing 22.5% External Quantum Efficiency for Solution-Processed
692   Thermally Activated Delayed-Fluorescence OLEDs with Red Emission at 622 nm via a
693   Synergistic Strategy of Molecular Engineering and Host Selection. *Advanced Materials* **0**,
694   1901404, doi:10.1002/adma.201901404.
695 51   Wong, M. Y. & Zysman-Colman, E. Purely Organic Thermally Activated Delayed Fluorescence
696   Materials for Organic Light-Emitting Diodes. *Advanced Materials* **29**, 1605444,
697   doi:10.1002/adma.201605444 (2017).
698 52   Dias, F. B. *et al.* The Role of Local Triplet Excited States and D-A Relative Orientation in
699   Thermally Activated Delayed Fluorescence: Photophysics and Devices. *Advanced Science* **3**,
700   1600080, doi:10.1002/advs.201600080 (2016).
701 53   Etherington, M. K., Gibson, J., Higginbotham, H. F., Penfold, T. J. & Monkman, A. P. Revealing
702   the spin–vibronic coupling mechanism of thermally activated delayed fluorescence. *Nature*
703   *Communications* **7**, 13680, doi:10.1038/ncomms13680

704   http://www.nature.com/articles/ncomms13680#supplementary-information (2016).
705 54   Samanta, P. K., Kim, D., Coropceanu, V. & Brédas, J.-L. Up-Conversion Intersystem Crossing
706   Rates in Organic Emitters for Thermally Activated Delayed Fluorescence: Impact of the
707   Nature of Singlet vs Triplet Excited States. *J. Am. Chem. Soc.* **139**, 4042-4051,
708   doi:10.1021/jacs.6b12124 (2017).
709 55   Noda, H. *et al.* Critical role of intermediate electronic states for spin-flip processes in charge-
710   transfer-type organic molecules with multiple donors and acceptors. *Nature Materials* **18**,
711   1084-1090, doi:10.1038/s41563-019-0465-6 (2019).
712 56   Nakanotani, H. *et al.* High-efficiency organic light-emitting diodes with fluorescent emitters.
713   *Nature Communications* **5**, 4016, doi:10.1038/ncomms5016

714   https://www.nature.com/articles/ncomms5016#supplementary-information (2014).
715 57   Pershin, A. *et al.* Highly emissive excitons with reduced exchange energy in thermally
716   activated delayed fluorescent molecules. *Nature Communications* **10**, 597,
717   doi:10.1038/s41467-019-08495-5 (2019).
718 58   Hatakeyama, T. *et al.* Ultrapure Blue Thermally Activated Delayed Fluorescence Molecules:
719   Efficient HOMO–LUMO Separation by the Multiple Resonance Effect. *Advanced Materials*
720   **28**, 2777-2781, doi:10.1002/adma.201505491 (2016).
721 59   Kondo, Y. *et al.* Narrowband deep-blue organic light-emitting diode featuring an
722   organoboron-based emitter. *Nature Photonics*, doi:10.1038/s41566-019-0476-5 (2019).
723 60   Di, D. *et al.* High-performance light-emitting diodes based on carbene-metal-amides. *Science*
724   **356**, 159-163, doi:10.1126/science.aah4345 (2017).
725 61   Hamze, R. *et al.* Eliminating nonradiative decay in Cu(I) emitters: >99% quantum
726   efficiency and microsecond lifetime. *Science* **363**, 601-606, doi:10.1126/science.aav2865
727   (2019).
728 62   Freeman, D. M. E. *et al.* Synthesis and Exciton Dynamics of Donor-Orthogonal Acceptor
729   Conjugated Polymers: Reducing the Singlet–Triplet Energy Gap. *J. Am. Chem. Soc.* **139**,
730   11073-11080, doi:10.1021/jacs.7b03327 (2017).

731 63 Schweicher, G., D'Avino, G., Ruggiero, M. T., Harkin, D. J., Broch, K., Venkateshvaran, D., Liu,
732   G., et al. . Chasing the 'Killer' Phonon Mode for the Rational Design of Low Disorder, High
733   Mobility Molecular Semiconductors. *Advanced Materials*, doi:
734   https://doi.org/10.1002/adma.201902407 (2019).
735 64 Rivnay, J. *et al.* Structural control of mixed ionic and electronic transport in conducting
736   polymers. *Nature Communications* **7**, 11287, doi:10.1038/ncomms11287

737 https://www.nature.com/articles/ncomms11287#supplementary-information (2016).
738 65 Someya, T., Bao, Z. & Malliaras, G. G. The rise of plastic bioelectronics. *Nature* **540**, 379-385,
739   doi:10.1038/nature21004 (2016).
740 66 Giovannitti, A. *et al.* Controlling the mode of operation of organic transistors through side-
741   chain engineering. *Proc Natl Acad Sci U S A* **113**, 12017-12022,
742   doi:10.1073/pnas.1608780113 (2016).
743 67 Nielsen, C. B. *et al.* Molecular Design of Semiconducting Polymers for High-Performance
744   Organic Electrochemical Transistors. *J Am Chem Soc* **138**, 10252-10259,
745   doi:10.1021/jacs.6b05280 (2016).
746 68 Leeuw, D. M. d., Simenon, M. M. J., Brown, A. R. & Einerhand, R. E. F. Stability of n-type
747   doped conducting polymers and consequences for polymeric microelectronic devices.
748   *Synthetic Metals* **87**, 53-59 (1997).
749 69 Giovannitti, A. *et al.* N-type organic electrochemical transistors with stability in water. *Nat
750   Commun* **7**, 13066, doi:10.1038/ncomms13066 (2016).
751 70 Sun, H. *et al.* Complementary Logic Circuits Based on High-Performance n-Type Organic
752   Electrochemical Transistors. *Advanced Materials* **30**, 1704916,
753   doi:10.1002/adma.201704916 (2018).
754 71 Yao, H. *et al.* 14.7% Efficiency Organic Photovoltaic Cells Enabled by Active Materials with a
755   Large Electrostatic Potential Difference. *Journal of the American Chemical Society* **141**, 7743-
756   7750, doi:10.1021/jacs.8b12937 (2019).
757 72 Peng, Q., Obolda, A., Zhang, M. & Li, F. Organic Light-Emitting Diodes Using a Neutral π
758   Radical as Emitter: The Emission from a Doublet. *Angewandte Chemie International Edition*
759   **54**, 7091-7095, doi:10.1002/anie.201500242 (2015).
760 73 Ai, X. *et al.* Efficient radical-based light-emitting diodes with doublet emission. *Nature* **563**,
761   536-540, doi:10.1038/s41586-018-0695-9 (2018).
762 74 Nagata, R., Nakanotani, H., Potscavage Jr., W. J. & Adachi, C. Exploiting Singlet Fission in
763   Organic Light-Emitting Diodes. *Advanced Materials* **30**, 1801484,
764   doi:10.1002/adma.201801484 (2018).
765 75 Salehi, A. *et al.* Realization of high-efficiency fluorescent organic light-emitting diodes with
766   low driving voltage. *Nature Communications* **10**, 2305, doi:10.1038/s41467-019-10260-7
767   (2019).
768 76 Kimura, K. *et al.* Selective triplet exciton formation in a single molecule. *Nature* **570**, 210-
769   213, doi:10.1038/s41586-019-1284-2 (2019).
770 77 Di, D. *et al.* Efficient Triplet Exciton Fusion in Molecularly Doped Polymer Light-Emitting
771   Diodes. *Advanced Materials* **29**, 1605987, doi:10.1002/adma.201605987 (2017).
772 78 Onwubiko, A. *et al.* Fused electron deficient semiconducting polymers for air stable electron
773   transport. *Nature Communications* **9**, 416, doi:10.1038/s41467-018-02852-6 (2018).

774